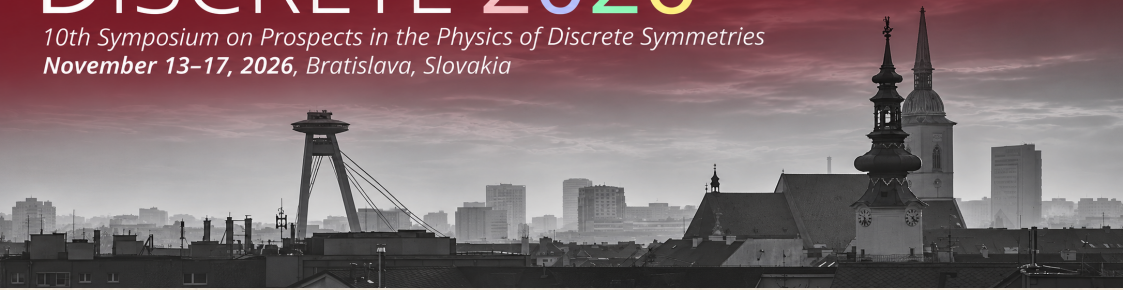
DISCRETE 2026
10th Symposium on Prospects in the Physics of Discrete Symmetries
***November 13–17, 2026**, Bratislava, Slovakia*



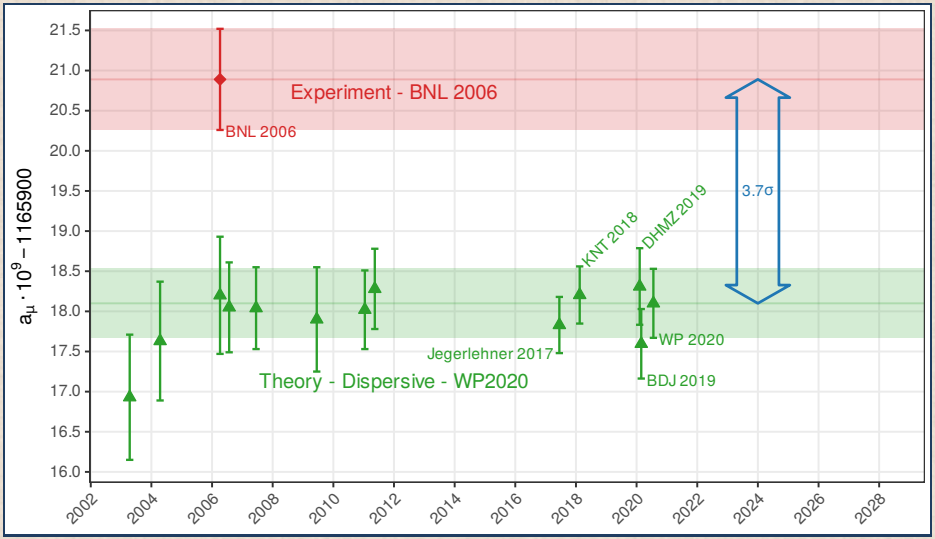
Final result of the Muon g-2 measurement at FNAL

Alberto Lusiani
Scuola Normale Superiore and INFN, sezione di Pisa
on behalf of the FNAL Muon g-2 collaboration



Fermilab

FNAL Muon g-2 project (E989) motivation



- BNL 2006: BNL-E821 Muon $g-2$ collaboration final report, Phys. Rev. D 73, 072003
- WP 2020: Muon $g-2$ theory initiative White Paper, Phys. Rept. 887 (2020) 1

Motion and spin precession of μ^+ in a uniform magnetic field

μ^+ spin precession relative to momentum

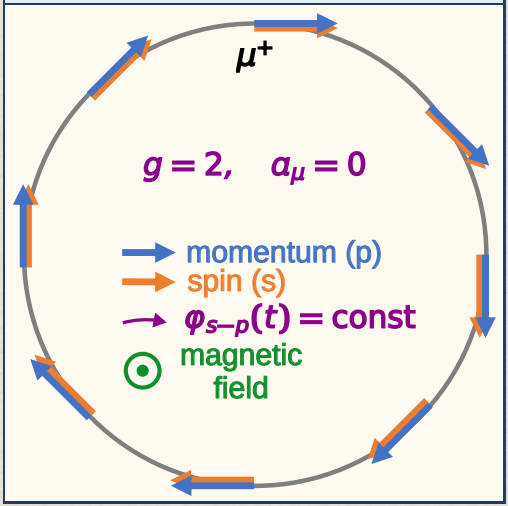
$$\vec{\omega}_s \quad - \quad \vec{\omega}_c \quad = \quad \vec{\omega}_a$$

$$\boxed{-g_\mu \frac{e\vec{B}}{2m_\mu c} - (1-\gamma)\frac{e\vec{B}}{m_\mu \gamma c}} \quad \boxed{-\frac{e\vec{B}}{m_\mu \gamma c}} \quad = \quad \boxed{-a_\mu \frac{e\vec{B}}{m_\mu c}}$$

Larmor + Thomas precessions | cyclotron frequency | no γ!

- frequency measurements best for precision
- NMR magnetic-field measurement also measures a frequency
- angle between momentum and spin: $\varphi(t) = \omega_a t$

polarized μ^+ in magnetic storage ring



Motion and spin precession of μ^+ in a uniform magnetic field

μ^+ spin precession relative to momentum

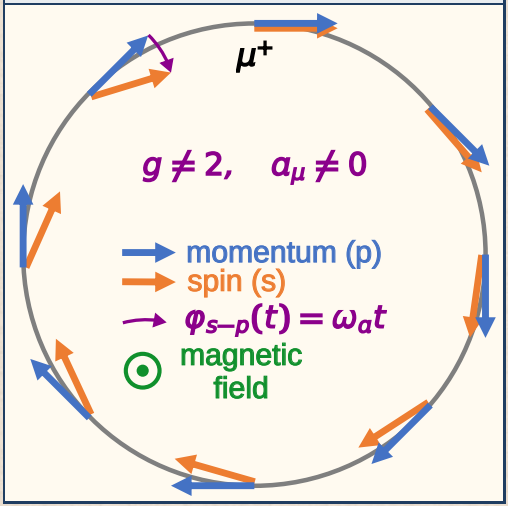
$$\vec{\omega}_s \quad - \quad \vec{\omega}_c \quad = \quad \vec{\omega}_a$$

$$\boxed{-g_\mu \frac{e\vec{B}}{2m_\mu c} - (1-\gamma)\frac{e\vec{B}}{m_\mu \gamma c}} \quad - \quad \boxed{-\frac{e\vec{B}}{m_\mu \gamma c}} \quad = \quad \boxed{-a_\mu \frac{e\vec{B}}{m_\mu c}}$$

Larmor + Thomas precessions | cyclotron frequency | no γ!

- frequency measurements best for precision
- NMR magnetic-field measurement also measures a frequency
- angle between momentum and spin: $\varphi(t) = \omega_a t$

polarized μ^+ in magnetic storage ring



Muon g-2 measurement at magic muon momentum

μ^+ precession

- accounting for vertical-focusing electric field and vertical muon beam oscillations:

$$\vec{\omega}_a \equiv \vec{\omega}_s - \vec{\omega}_c = \frac{-e}{m_\mu c}\left[a_\mu \vec{B} - \left(a_\mu - \left[\frac{m_\mu c}{p}\right]^2\right)\vec{\beta}\times\vec{E} - a_\mu\left(\frac{\gamma}{\gamma+1}\right)(\vec{\beta}\cdot\vec{B})\vec{\beta}\right]$$

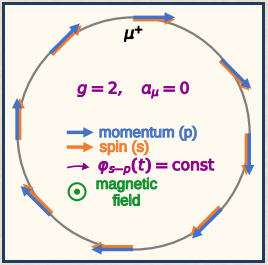
- zero $\vec{\beta}\times\vec{E}$ term $\Rightarrow$ $p_{\text{magic}} = \dfrac{m_\mu c}{\sqrt{a_\mu}} \approx 3.094\,\text{GeV}/c$, Lorentz $\gamma_{\text{magic}} \approx 29.3$
- muon spin precession $\omega_s \approx g_\mu \dfrac{eB}{2m_\mu c} + (1-\gamma)\dfrac{eB}{\gamma m_\mu c} \approx 2\pi \cdot 6.9\,\text{MHz}$

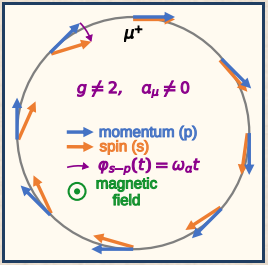
  muon cyclotron $\omega_c \approx \dfrac{eB}{\gamma m_\mu c} \approx 2\pi \cdot 6.7\,\text{MHz}$

  muon anomalous precession $\omega_a \approx a_\mu \dfrac{eB}{m_\mu c} \approx 2\pi \cdot 229\,\text{kHz}$

  proton spin precession $\omega_p'(T) \approx g_p'(T)\dfrac{eB}{2m_p c} \approx 2\pi \cdot 61.8\,\text{MHz}$
- ω_a independent (not directly dependent) of uncertainty on muon momentum / γ

magic momentum setup used since 1969 at CERN





FNAL-E989 project goals

FNAL-E989 design precision, compared to BNL-E821 final report (2006)

	BNL E821 (2006)	FNAL E989 final goal	
ω_a statistical	460 ppb	100 ppb	$\times$21 detected muon decays ($1.6{\cdot}10^{11}$)
ω_a systematic	210 ppb	70 ppb	faster calorimeter with laser calibration, tracker
ω_p systematic	170 ppb	70 ppb	more uniform B, improve NMR measurement
external measurements	25 ppb	25 ppb	
total	540 ppb	140 ppb	

ω_a: measured muon spin precession frequency in magnetic field
ω_p: measured proton spin precession frequency to measure magnetic field

FNAL Muon $g-2$ collaboration

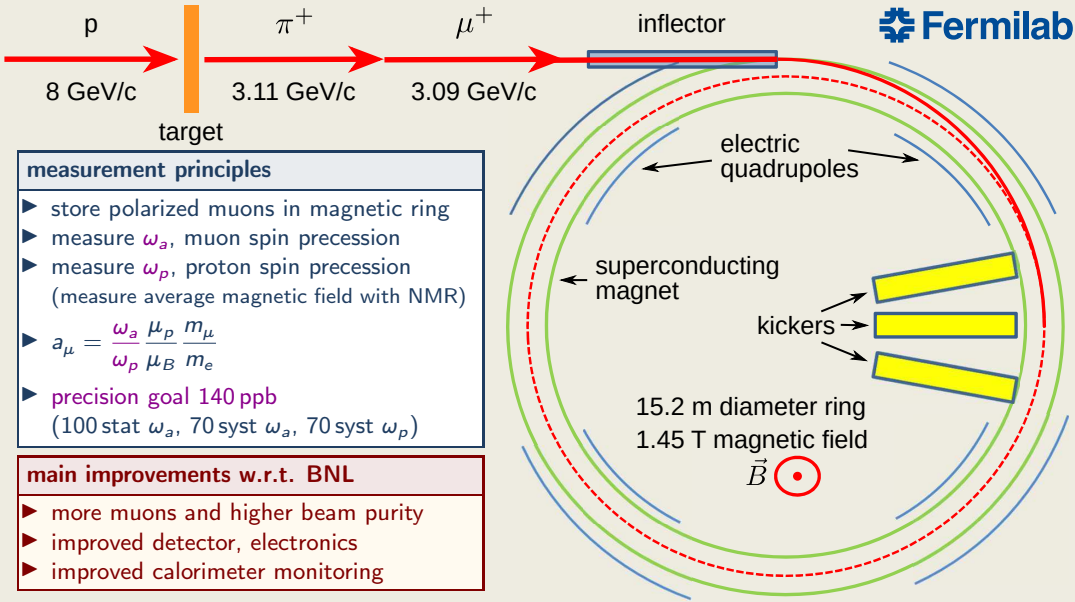


176 collaborators, 34 institutes, 7 countries

Particle-, Nuclear-, Atomic-, Optical-, Accelerator-,
and Theoretical-Physicists and Engineers

[some faces at unblinding meeting of 20 May 2025, by P.Winter, CERN, Jun 2025]

Muon g-2 measurement technique



measurement principles

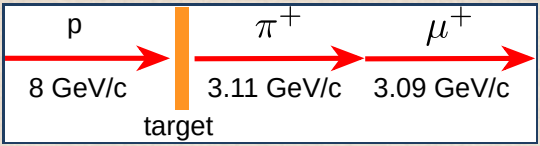
- store polarized muons in magnetic ring
- measure ω_a, muon spin precession
- measure ω_p, proton spin precession
  (measure average magnetic field with NMR)
- $a_\mu = \frac{\omega_a}{\omega_p} \frac{\mu_p}{\mu_B} \frac{m_\mu}{m_e}$
- precision goal 140 ppb
  (100 stat ω_a, 70 syst ω_a, 70 syst ω_p)

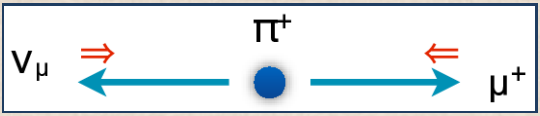
main improvements w.r.t. BNL

- more muons and higher beam purity
- improved detector, electronics
- improved calorimeter monitoring

Production of polarized muons

- dump 8 GeV protons on target to produce pions
- select pions with momentum $p \simeq 3.11\,\mathrm{GeV}/c$
- let them decay into muons
- in pion rest frame, parity violation in pion decay makes the μ^+ spin antiparallel to its momentum
- in laboratory frame, highest-energy muons are >90% polarized

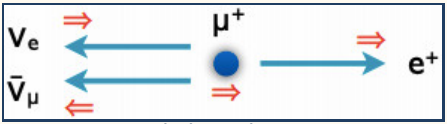




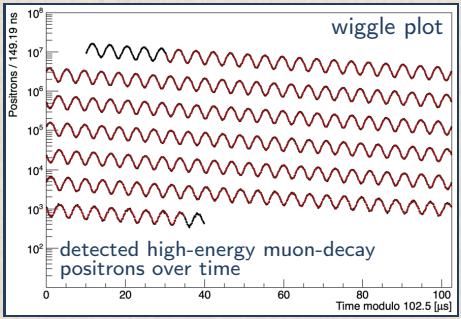
- with 8 GeV protons on target, μ^+ are produced more frequently than μ^-

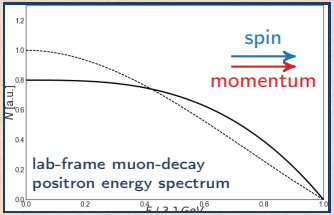
Rate of high-energy muon-decay positrons modulated with $\cos \omega_a t$

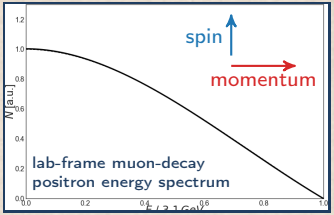
- parity violation favors high-energy positrons emitted along the muon spin

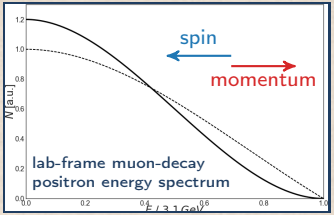


- positrons emitted along the muon momentum have highest energy in laboratory frame
- $N_e(E_e > E_t) = N_{e0} e^{-t/\tau_\mu}(1 + A \cos \omega_a t)$

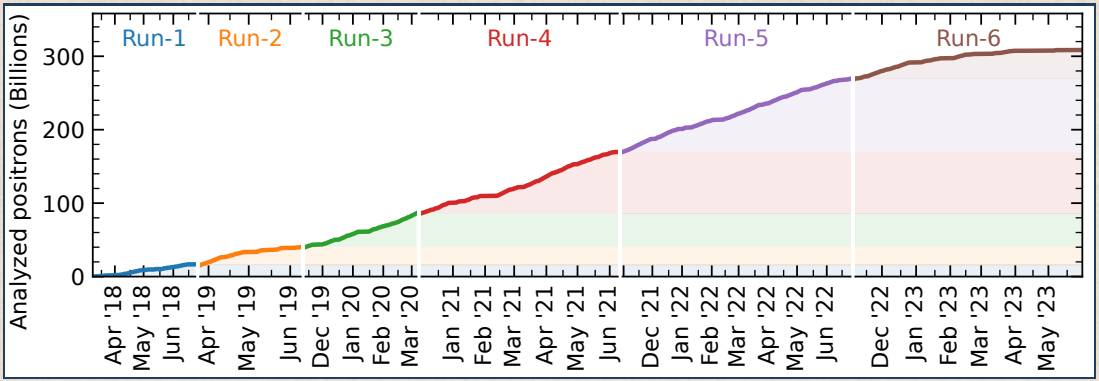








FNAL Muon g-2 experiment data samples



- ∼5000 stored muons per fill, 12 Hz fills
- ∼500 high-energy positrons detected per fill
- ∼310 billion analyzed high-energy positrons from muon decays

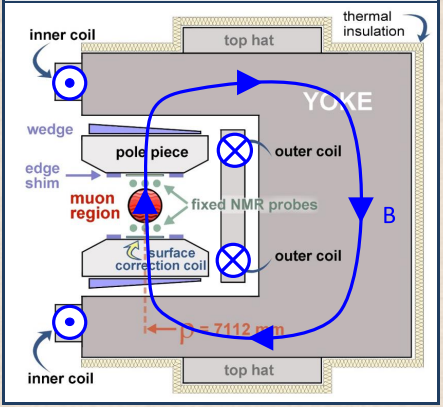
FNAL measurements

sample	publication
Run-1	April 2021
Run-2/3	August 2023
Run-4/5/6	June 2025

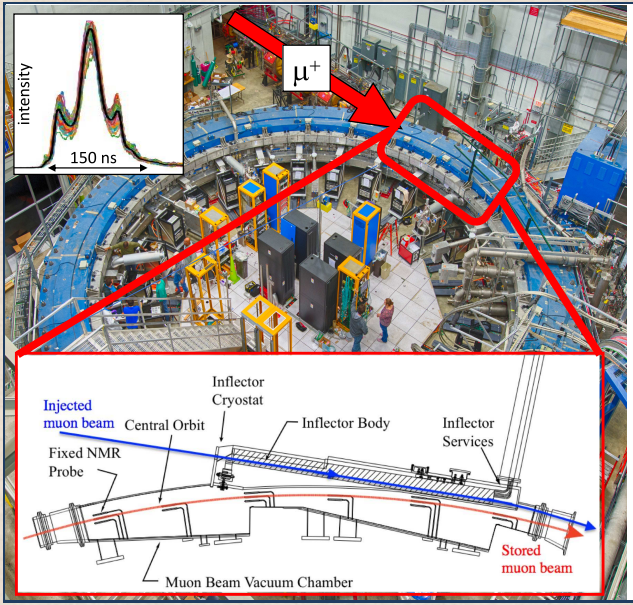
FNAL accelerator complex for Muon $g-2$



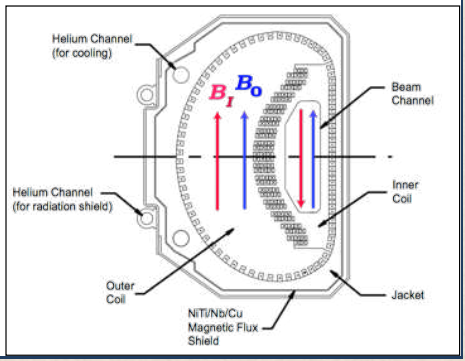
section of muon g-2 storage ring magnet



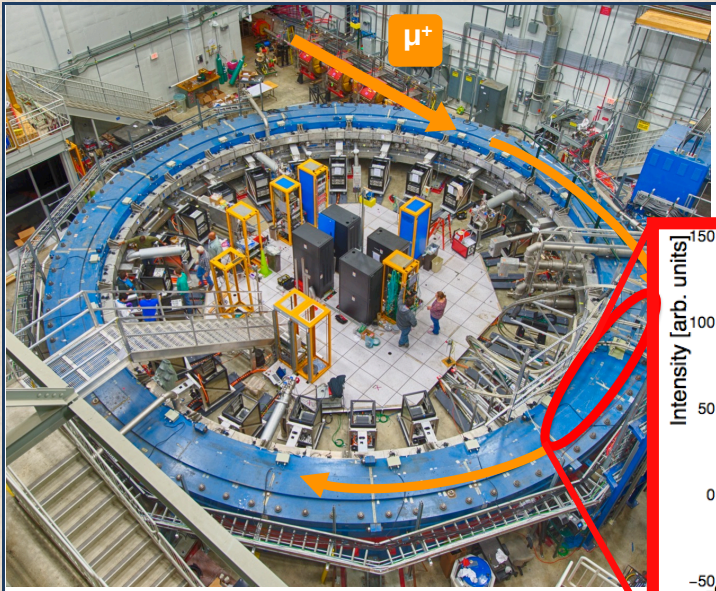
Pulsed inflector magnet injects muons into storage ring



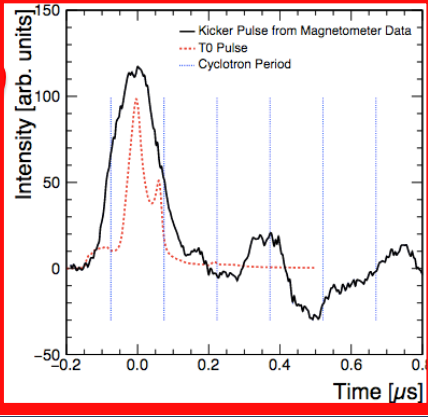
- cancels 1.45 T field in beam channel
- minimal perturbation of magnetic field in muon storage volume



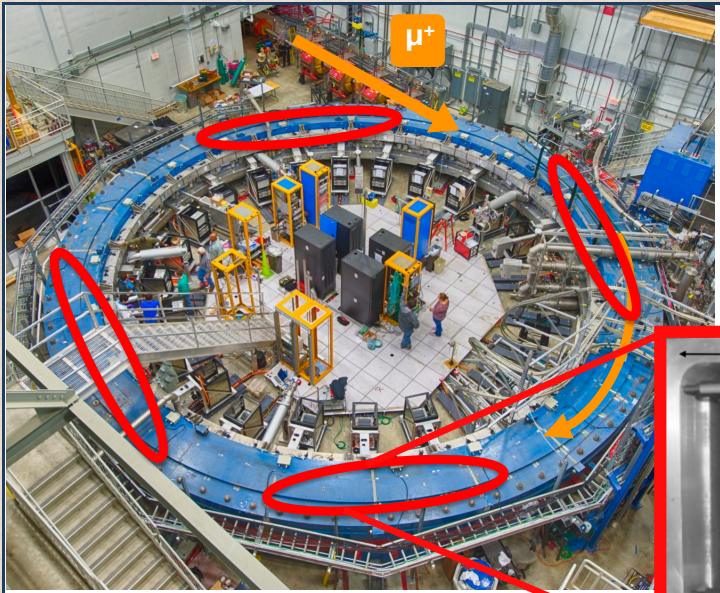
Magnetic kickers put muons into correct orbit



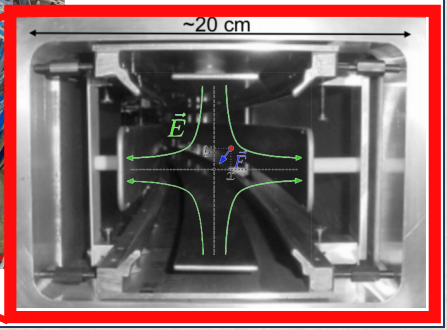
- 3 pulsed electromagnets
- ∼220 G magnetic field
- 3 – 4 kA peak current
- ∼130 ns pulse duration, shorter than cyclotron period (149.2 ns)



Electric quadrupoles focus beam vertically

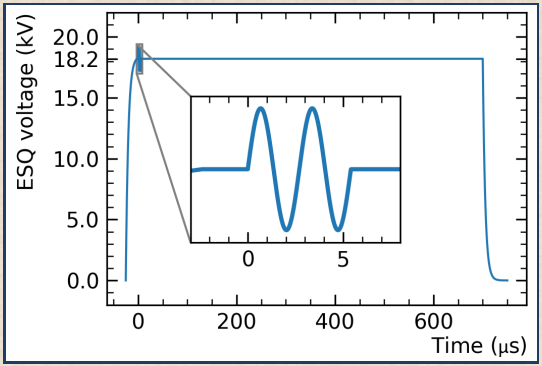


- operated at voltages of $\pm(15\text{–}21)$ kV
- pulsed to avoid space-charge accumulation



Run 4/5/6: RF on quad HV to dampen radial & vertical beam dynamics

- ∼1 kV radio-frequency modulation of quad high voltage in first 6 μs of quad activation during fills
  - obtained significant reduction of radial & vertical motion of average muon distribution
  - ∼10× ω_a bias reduction when not accounting for beam dynamics

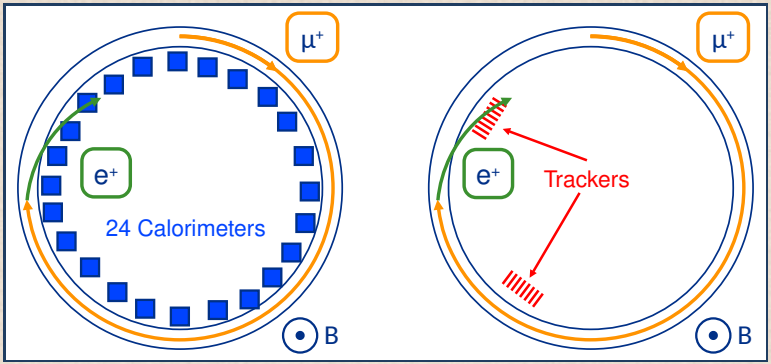


four datasets with different RF damping / Run

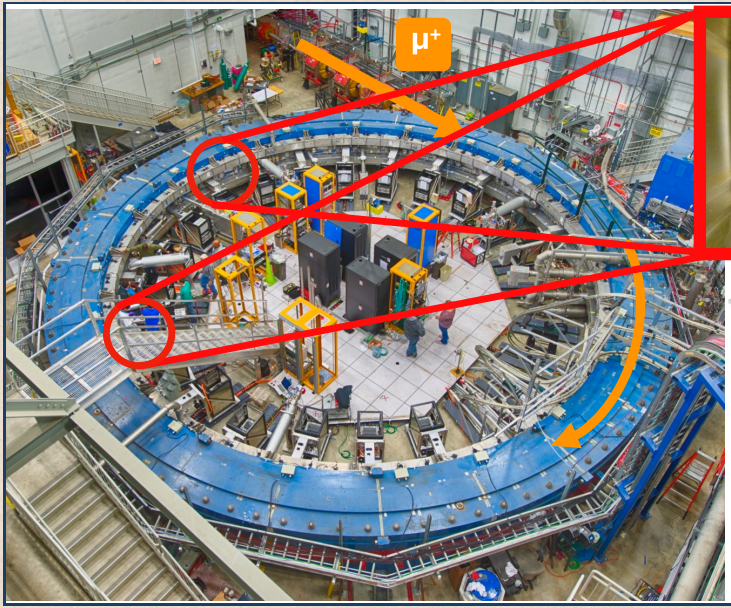
dataset	RF damping on beam oscillations
NoRF	none
xRF	radial only
xyRF5	radial & vertical, Run 5
xyRF6	radial & vertical, Run 6

Positrons from positive-muon decays are detected

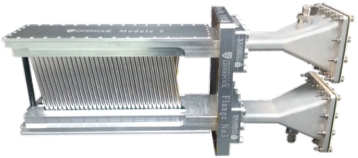
- positrons from positive-muon decays curl inward and are detected
- calorimeters measure energy for ω_a measurement
- trackers reconstruct muon decay vertices to measure beam dynamics



Two tracking stations



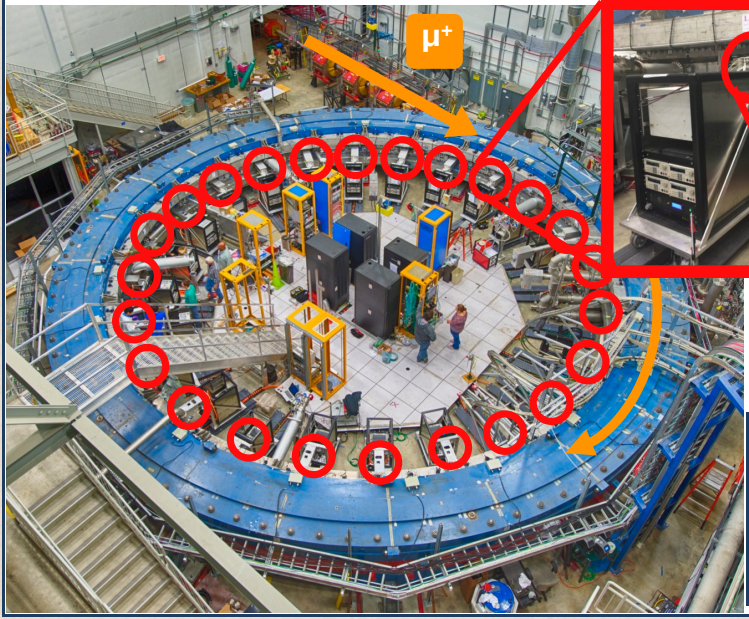


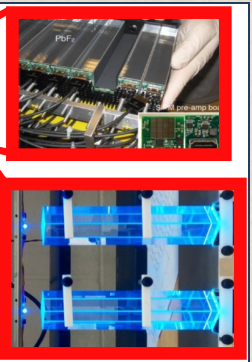


each tracker

- 8 modules
- 128 straw chambers each
- trace back muon decay points

24 calorimeter modules





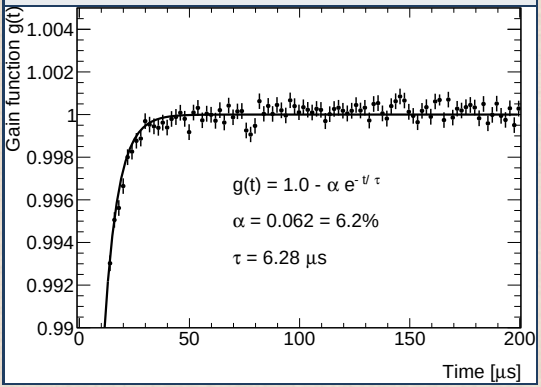
each module

- 6×9 array of PbF_2 crystals
- 2.5 cm×2.5 cm×14 cm, 15 X_0
- read out Cherenkov light at 800 MHz with SiPMs
- continuous gain monitoring with laser system pulses

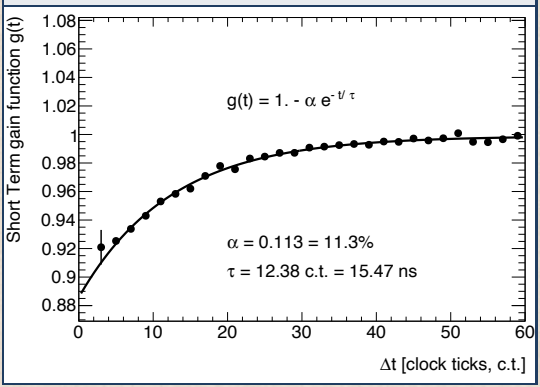
Laser calorimeter gain monitoring system

- SiPM gain is reduced by occurrence of preceding hits
- if uncorrected, sizeable bias in ω_a measurement
- gain monitored by reading back reference laser light pulses injected in calorimeter PbF_2 crystals
  - also during data-taking
- positron energy measurement from SiPM readout corrected for average measured gain loss

μs time scale SiPM power supply recovery time

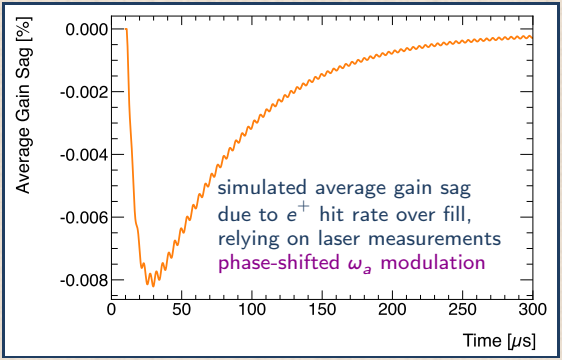


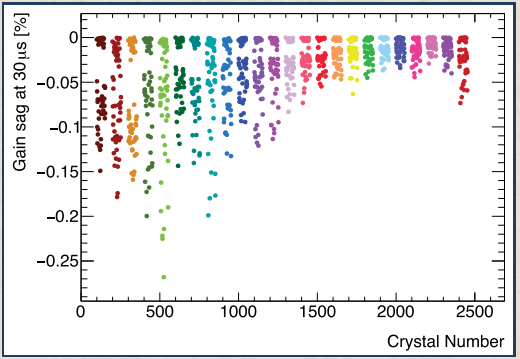
ns time scale SiPM pixel recovery time



Positron-rate-dependent calorimeter gain sag

- SiPM-recovery-time calorimeter gain sag
  - injection beam flash, 0.008% average effect, measured
  - time-dependent positron hit rate, much smaller, inferred





phase-shifted varying amplitude ω_a gain modulation

- below sensitivity of laser monitoring system during data-taking
- dedicated studies estimated ∼40 ppb bias on measured ω_a^m
- extra studies performed with laser pulses after end of data-taking
- estimated biases subtracted for Run 4/5/6 2025 release PRL paper
  - published Run 1 & 2/3 values and uncertainties revised

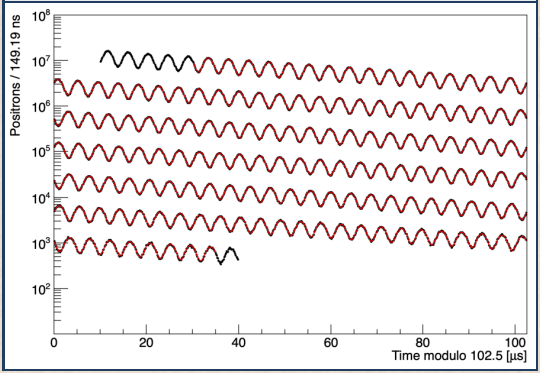
ω_a^m wiggle plot fit, 5-parameter function

$$N(t) = N_0 e^{-t/\tau_\mu} [1 + A\cos(\omega_a t + \varphi)]$$

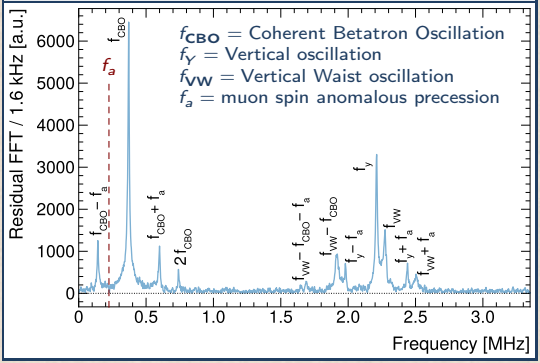
- $N(t)$: number of e^+ vs. time
- N_0: normalization
- τ_μ: dilated μ^+ lifetime
- A: wiggle asymmetry
- ω_a: anomalous precession frequency
- φ: average spin phase at injection

- peaks in Fourier transform of fit residuals
- biases of order 1 ppm

wiggle plot



Fourier transform of wiggle plot fit residuals



ω_a^m wiggle plot fit, full function

- ~30-parameter typical fit function to account for
  - beam vertical and horizontal/radial motion
  - muon loss
- no peaks in Fourier transform of fit residuals
- good χ^2 [dataset with the most statistics $\chi^2/\text{ndof} = 4007/4097$, $p = 84\%$]

example full ω_a fit function

$$N_0\, e^{-\frac{t}{\gamma\tau}}\,(1 + A\cdot A_{BO}(t)\cos(\omega_a t + \phi\cdot\phi_{BO}(t)))\cdot N_{\mathrm{CBO}}(t)\cdot N_{\mathrm{VW}}(t)\cdot N_y(t)\cdot N_{2\mathrm{CBO}}(t)\cdot J(t)$$

$$A_{\mathrm{BO}}(t) = 1 + A_A\cos(\omega_{\mathrm{CBO}}(t) + \phi_A)e^{-\frac{t}{\tau_{\mathrm{CBO}}}}$$

$$\phi_{\mathrm{BO}}(t) = 1 + A_\phi\cos(\omega_{\mathrm{CBO}}(t) + \phi_\phi)e^{-\frac{t}{\tau_{\mathrm{CBO}}}}$$

$$N_{\mathrm{CBO}}(t) = 1 + A_{\mathrm{CBO}}\cos(\omega_{\mathrm{CBO}}(t) + \phi_{\mathrm{CBO}})e^{-\frac{t}{\tau_{\mathrm{CBO}}}}$$

$$N_{2\mathrm{CBO}}(t) = 1 + A_{2\mathrm{CBO}}\cos(2\omega_{\mathrm{CBO}}(t) + \phi_{2\mathrm{CBO}})e^{-\frac{t}{2\tau_{\mathrm{CBO}}}}$$

$$N_{\mathrm{VW}}(t) = 1 + A_{\mathrm{VW}}\cos(\omega_{\mathrm{VW}}(t)t + \phi_{\mathrm{VW}})e^{-\frac{t}{\tau_{\mathrm{VW}}}}$$

$$N_y(t) = 1 + A_y\cos(\omega_y(t)t + \phi_y)e^{-\frac{t}{\tau_y}}$$

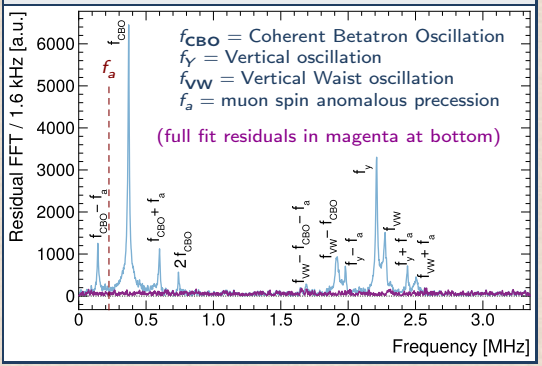
$$J(t) = 1 - k_{LM}\int_{t_0}^{t}\Lambda(t)dt$$

$$\omega_{\mathrm{CBO}}(t) = \omega_0 t + Ae^{-\frac{t}{\tau_A}} + Be^{-\frac{t}{\tau_B}}$$

$$\omega_y(t) = F\omega_{\mathrm{CBO}(t)}\sqrt{2\omega_c/F\omega_{\mathrm{CBO}}(t) - 1}$$

$$\omega_{\mathrm{VW}}(t) = \omega_c - 2\omega_y(t)$$

Fourier transform of wiggle plot fit residuals



Measuring ω_a^m with ∼30 ppb systematic accuracy for Run 4/5/6

- 5 independent and mutually software-blinded analysis groups
- completed total of 20 analyses (on each of 4 Run 4/5/6 datasets)
- consistency checks of SW and HW blind analyses
- consistency checks of common-HW-blinded analyses
- to estimate statistical correlations between analyses
  - assembled 200 bootstrap samples by resampling dataset subruns with replacement
  - estimated between-analyses correlations on data
  - bootstrap fits performed for most analyses
    (also done for a few analyses in the Run 2/3 measurement)
- perform one analysis fit on the wiggle plot assembled for another analysis
- all these tests either succeeded or facilitated debugging and well-understood fixes

ω_a^m measurement done separately on 4 datasets

- for each dataset, ω_a^m = arithmetic mean of 7 analyses using most precise methods
  - conservative 100% correlation assumed for each statistical and systematic uncertainty component
  - safe, stable, and only 1.5% larger uncertainty than optimal average

Run 4/5/6 ω_a measurements, 5 groups, 8 methods, 20 analyses

groups

g
BU
RE1
RE2
RE3
RE4
EU
Ky
SJTU

reconstructions

r
RW
RE
RI2
RQ

analyses

g	m	r	rq
BU	T, A, RT, RA	RW	K
RE1	T, A	RE	R
RE2	T, A	RE	
RE3	RT, RA	RE	R
RE4	ST, SA	RE	
EU	T, A, RT, RA	RI2	R
Ky	Q, RQ	RQ	R
SJTU	T, A	RW	

measurement methods

m	method
T	Threshold
A	Asymmetry weighted
RT	Ratio T
RA	Ratio A
Q	Charge
RQ	Ratio Charge
ST	Stroboscopic T
SA	Stroboscopic A

pileup subtraction

ps
RW-BU
RE
RW-EU
RW-SJTU

ratio quartering methods

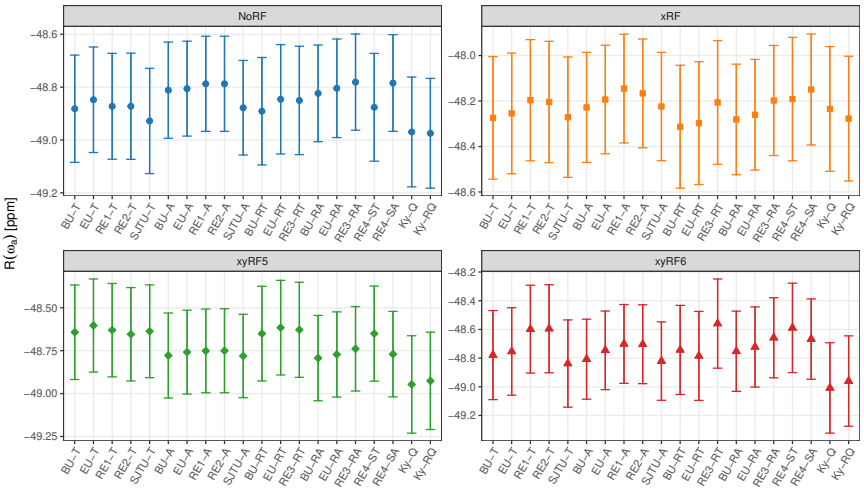
rq	ratio quartering methods
R	random
K	kernel

envelope modeling

em
analytic function
spline
Gaussian Process Regression

ω_a^m measurements must be consistent within each dataset

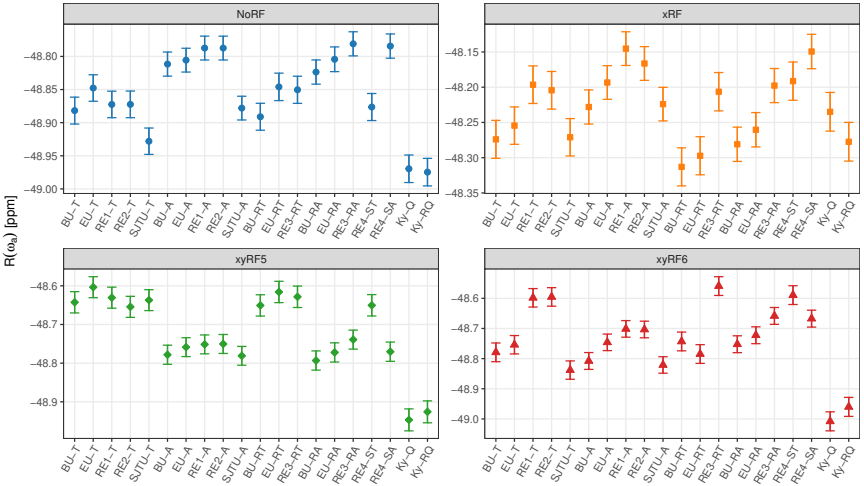
20 ω_a^m measurements on 4 Run 4/5/6 datasets



- however, statistical uncertainties within same datasets are highly correlated

ω_a^m measurements with only estimated systematic uncertainties

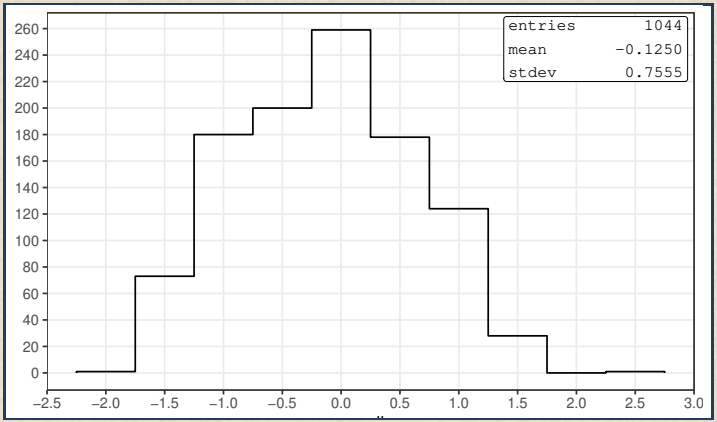
20 ω_a^m measurements on 4 Run 4/5/6 datasets



- even assuming uncorrelated systematics, ω_a^m measurements are inconsistent
- estimate variance-contributing statistical decorrelation between analyses using bootstrap samples

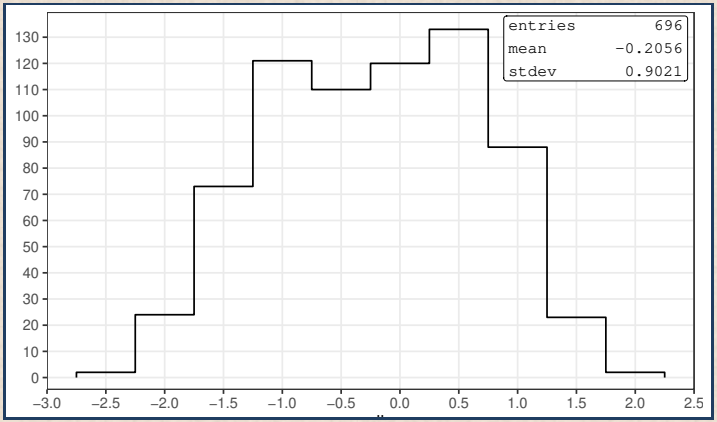
Pulls – dealing with analysis-group-dependent blinding offsets

- consistency checks for group-dependent blinding offsets possible relying on different datasets
- $\text{pull} = \dfrac{(\omega_a^{\text{dataset 2, analysis 2}} - \omega_a^{\text{dataset 2, analysis 1}}) - (\omega_a^{\text{dataset 1, analysis 2}} - \omega_a^{\text{dataset 1, analysis 1}})}{\sqrt{\sigma^2(\omega_a^{\text{dataset 2, analysis 2}} - \omega_a^{\text{dataset 2, analysis 1}}) + \sigma^2(\omega_a^{\text{dataset 1, analysis 2}} - \omega_a^{\text{dataset 1, analysis 1}})}}$



statistical decorrelation estimated with bootstrap samples

Pulls after removing group-dependent blinding offsets



statistical decorrelation estimated with bootstrap samples

Run 4/5/6 ω_a^m uncertainties

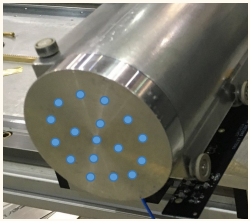
- many ω_a^m systematic effects have been studied

Category	NoRF (ppb)	xRF (ppb)	xyRF5 (ppb)	xyRF6 (ppb)
Statistical	182	241	246	277
CBO	22	19	20	24
Residual slow gain variation	22	20	16	11
Gain corrections	4	5	6	7
Pileup	6	6	6	5
Muon loss	2	3	3	3
Ratio method inputs	1	1	0	0
Randomization	1	2	2	2
Total systematic	32	29	27	28

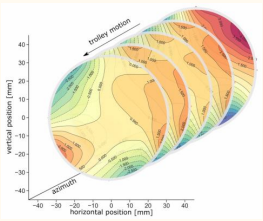
- averaged over the seven ω_a^m methods of Run 4/5/6 measurement

Measurement of the magnetic field map $\omega_p'(T_r)^m$

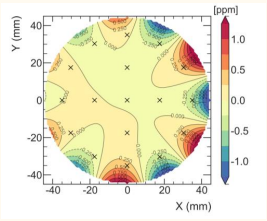
- in-vacuum trolley with NMR probes maps magnetic field every ∼3 days



trolley with 17 probes



2-D field maps (∼8000 points)

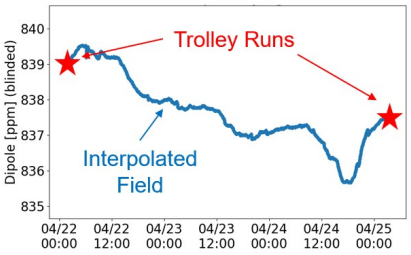


azimuthally averaged field map

- 378 fixed probes monitor field during muon storage at 72 locations

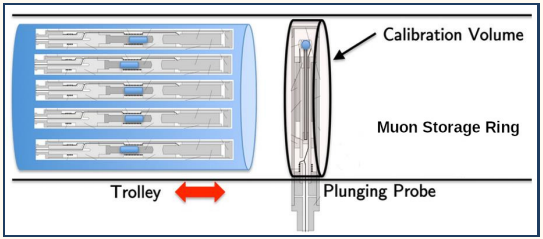
Fixed probes above/below muon storage region

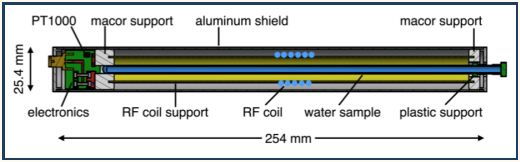


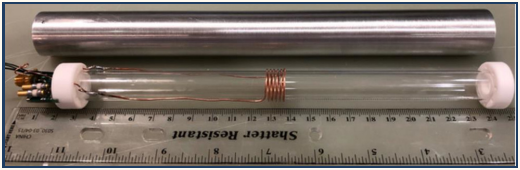


Measurement of the magnetic field, probe calibration

- calibrate petroleum-jelly trolley probes with cylindrical H_2O probe (plunging probe) in same physical positions [Run 4/5/6: 20 ppb consistency and reproducibility]







- calibrate plunging probe in ANL MRI magnet
  - reference spherical H_2O probe [Run 4/5/6: 15 ppb precision]
  - reference ^3He probe [Run 4/5/6: 20 ppb precision]

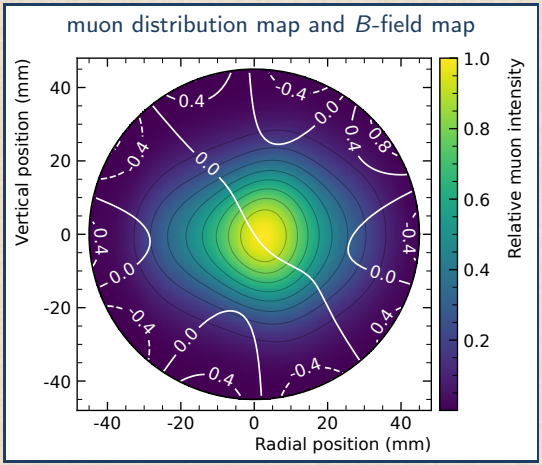


H_2O probe



^3He probe

Measurement of the magnetic field, weighting with muon distribution map M



- muon distribution map M reconstructed
  - with trackers – close to trackers
  - with trackers + simulation – elsewhere
- Run 4/5/6: 34 ppb systematic uncertainty

$\tilde{\omega}'_p(T_r)^m = \omega'_p(T_r)^m \otimes M$

- average of B-field map $[\omega'_p(T_r)^m]$ weighted with muon distribution map (M)
- Run 4/5/6: 48 ppb precision

$R'_\mu(T_r)$, corrections to ω_a^m and $\tilde{\omega}'_p(T_r)^m$

$$R'_\mu(T_r) = \frac{\omega_a}{\tilde{\omega}'_p(T_r)} = \frac{\omega_a^m}{\tilde{\omega}'_p(T_r)^m} \frac{1 + \overbrace{C_e + C_p + C_{\text{pa}} + C_{\text{dd}} + C_{\text{ml}}}^{\text{beam-dynamics corrections}}}{1 - \underbrace{B_k - B_q}_{\text{transient-fields corrections}}}$$

corrected: ω_a, $\tilde{\omega}'_p(T_r)$ — measured: ω_a^m, $\tilde{\omega}'_p(T_r)^m$

- C_e quadrupole electric field on muon distribution around magic radius
  - estimated by measuring muon radial distribution with calorimeters, trackers, and Miniscifi
- C_p (pitch) a_μ shift from muon vertical motion
  - estimated by measuring muon vertical distribution with trackers and beam dynamics simulation
- C_{pa} (phase acceptance) phase shift from time evolution of transverse muon decay position in det. acceptance
  - phase dependence with position estimated with simulation
  - evolution of muon transverse distribution measured with tracker and beam dynamics simulation
- C_{dd} (differential decay) phase shift from time evolution of muon ensemble average momentum
  - direct (from upstream beamline correlation phase - momentum)
  - transverse radial (muon decay kinematics phase shift, momentum correlation via beam acceptance)
  - transverse vertical (muon decay kinematics phase shift, momentum correlation via beam acceptance)
  - longitudinal (early arrival longer precession in magnetic field)
  - all components estimated with dedicated measurements and simulations
- C_{ml} (muon loss) time-dependent spectrum of lost muons
  - estimated by measuring muon loss

$R'_\mu(T_r)$, corrections to ω_a^m and $\tilde{\omega}'_p(T_r)^m$

$$R'_\mu(T_r) = \underbrace{\frac{\omega_a}{\tilde{\omega}'_p(T_r)}}_{\text{corrected}} = \underbrace{\frac{\omega_a^m}{\tilde{\omega}'_p(T_r)^m}}_{\text{measured}} \frac{1 + \overbrace{C_e + C_p + C_{\text{pa}} + C_{\text{dd}} + C_{\text{ml}}}^{\text{beam-dynamics corrections}}}{1 - \underbrace{B_k - B_q}_{\text{transient-fields corrections}}}$$

- B_k transient B-field generated by kicker eddy currents
  - estimated using dedicated measurements of transient field
- B_q transient B-field from vibration of plates of pulsed electrostatic quadrupole field system
  - estimated using dedicated measurements of transient field

Calculation of the muon magnetic anomaly a_μ

$$a_\mu = R'_\mu(T_r) \cdot \frac{\mu'_{\mathrm{p}}(T_r)}{\mu_{\mathrm{B}}} \frac{m_\mu}{m_{\mathrm{e}}}$$

- $R'_\mu(T_r)$ Muon g-2 collaboration measurement that enters the CODATA fits
- $\frac{\mu'_{\mathrm{p}}(T_r)}{\mu_{\mathrm{B}}}$ proton magnetic moment in a spherical water sample at $T_r = 25\,^\circ\mathrm{C}$, in Bohr magnetons CODATA 2022
- $\frac{m_\mu}{m_{\mathrm{e}}}$ ratio of muon to electron mass CODATA 2022

notes

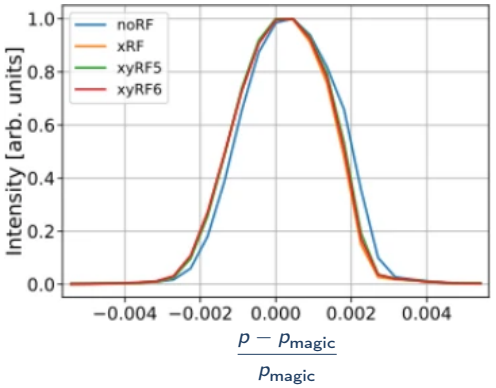
- since 2025 using CODATA ref. temperature, to profit from improved CODATA 2022 $\mu'_{\mathrm{p}}(T_r)/\mu_{\mathrm{B}}$
- all BNL, FNAL Run 1, FNAL Run 2/3 ω_p, $\tilde{\omega}'_p(T_r)$ recomputed at $T_r = 25\,^\circ\mathrm{C}$ and a_μ's recomputed

E-field correction C_e: largest one & largest systematic contribution

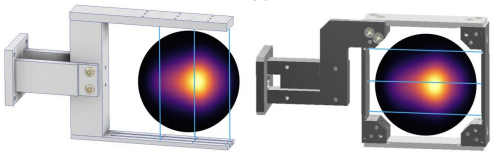
depends on radial muon distribution,
equivalent to momentum distribution,
obtained with three detectors:

- calorimeters
  - parasitic on data-taking
  - measure injected muon bunches dephasing (how muons spread along the beam over time)
  - improved fits for Run 2/3 release
  - much improved fits for Run 4/5/6 release
- trackers
  - parasitic on data-taking
  - complement with beam dynamics simulation
  - measure muon radial distribution along ring
- Miniscifi (Minimally Intrusive Scintillating Fiber detector) (Run 4/5/6)
  - dedicated runs
  - complement with beam dynamics simulation
  - measure muon radial distribution

measured muon momentum distribution

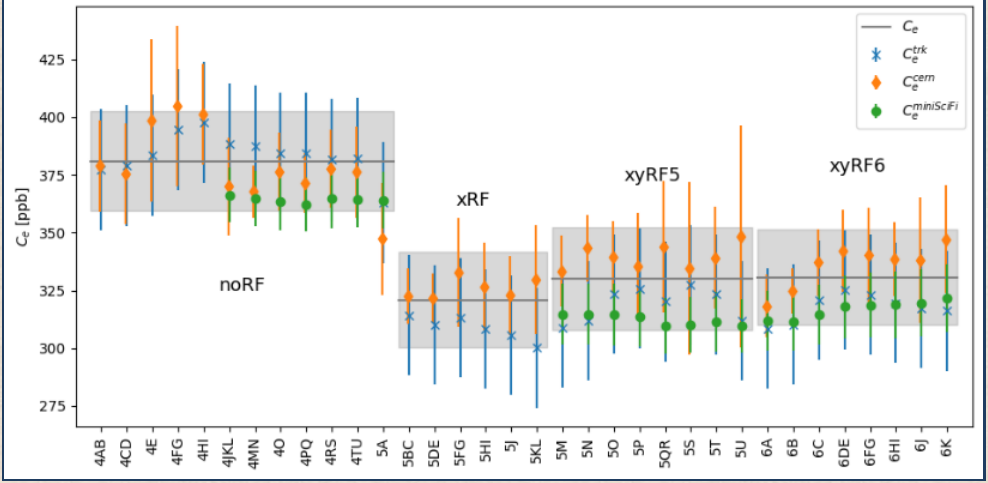


Miniscifi



E-field correction C_e: largest one & largest systematic contribution

Run 4/5/6: 3 different measurements are consistent

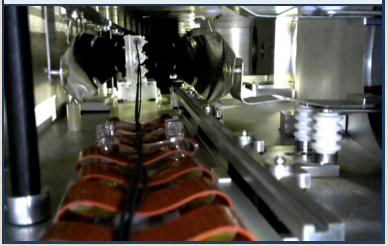


- Run 4/5/6 ω_a correction: 347 ± 27 ppb

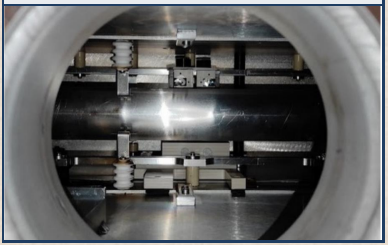
Kicker transient field measured with two magnetometers (Run 4/5/6)

- measure Faraday rotation of polarized laser light in TGG crystal
- Run 4/5/6 improvements:
  - two independent teams and detectors
  - higher transient field measured off magic-radius
  - checks with hardware mockup
  - improved understanding ⇒ revised Run 1, 2/3 results
- Run 4/5/6 correction to $\omega_p'(T_r)^m$: -37 ± 22 ppb

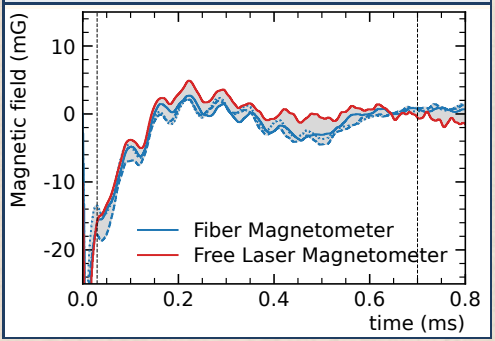
fiber magnetometer



free laser magnetometer

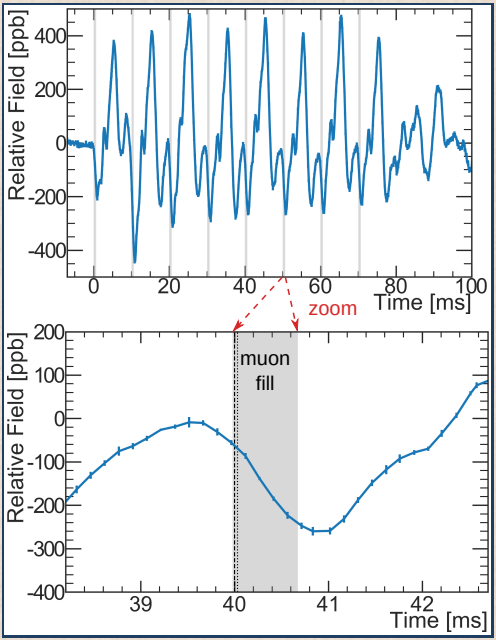


kicker transient *B* field



B_q correction for transient B field produced by electric quadrupoles

- electric quadrupoles are pulsed (to prevent static charge accumulation)
- vibration of the conductive plates perturbs magnetic field
- special NMR probes measure the transient field perturbation in muon region
- improved spatial coverage in Runs after Run 1
- Run 4/5/6 correction to $\omega_p'(T_r)^m$: -21 ± 20 ppb



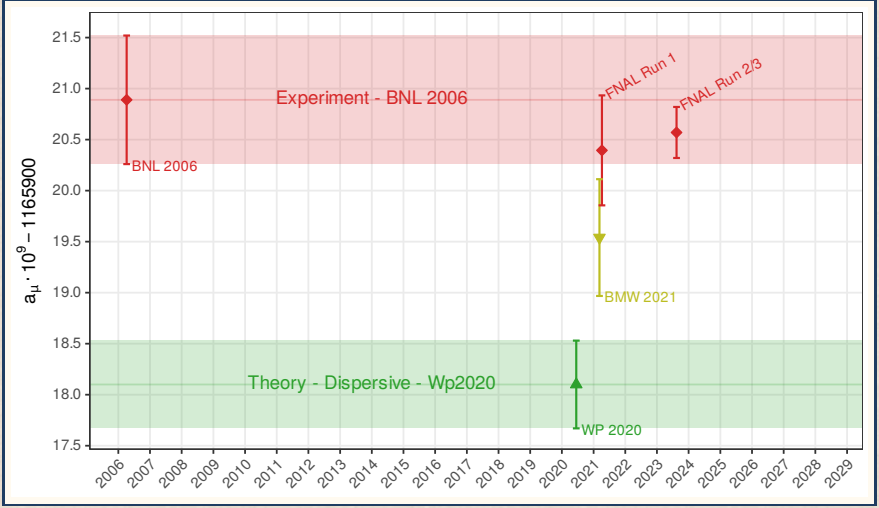
Revisions of Run 1 and Run 2/3 [ppb]

	rev. Run 1 Corr	Run 1 Unc	rev. Run 2/3 Corr	Run 2/3 Unc	Run 1..6 Corr	Run 1..6 Unc
ω_a^m (statistical)					···	98
ω_a^m (systematic)	+50	⊕28	+47	⊕24	···	32
C_e					374	28
C_p					174	10
C_{pa}					-34	15
C_{dd}			+32	⊕14	24	26
C_{ml}						3
$\omega_p'(T_r)^m$ (mapping, tracking)					···	33
$\omega_p'(T_r)^m$ (calibration)					···	33
B_k			+19	⊕23	37	23
B_q					21	21
$\mu_p'(T_r)/\mu_B$					···	4
m_μ/m_e					···	22
Total systematic for $R_\mu'(T_r)$	+50	⊕28	+98	⊕36	596	78

correction	Run	effect
ω_a^m (systematic)	1, 2/3	rate-dependent gain sag
$C_{\text{dd-beamline}}$	2/3	wrong sign corrected
B_k	2/3	improved measurements of spatial variation

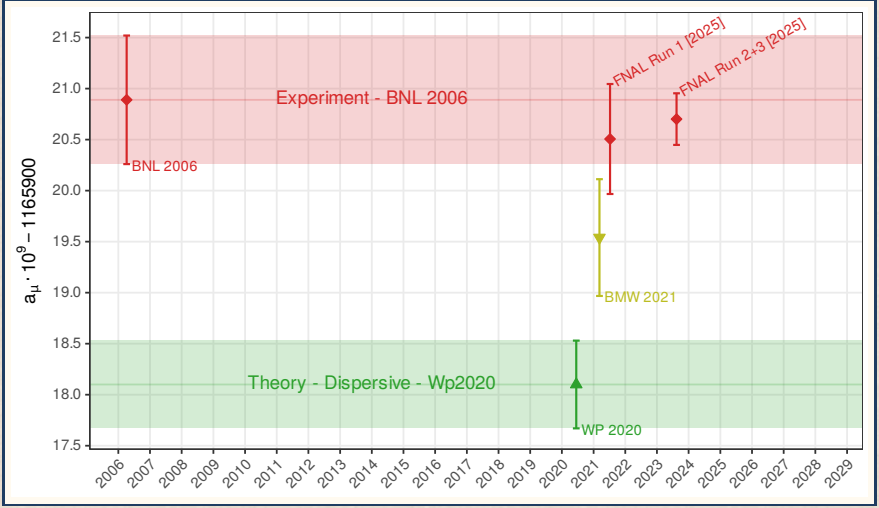
Revision of published Run 1 and Run 2/3 results in Sep 2025 PRL

published in 2021, 2023



Revision of published Run 1 and Run 2/3 results in Sep 2025 PRL

revised in Sep 2025

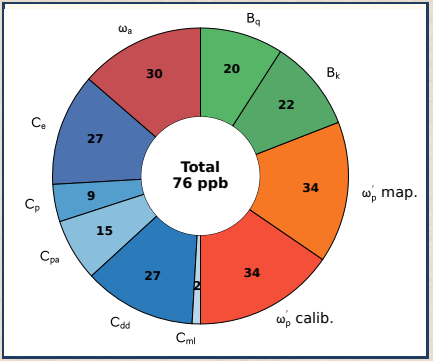


Systematic corrections and uncertainties for Run 4/5/6

Quantity	Correction (ppb)	Uncertainty (ppb)
ω_a^m (statistical)	···	114
ω_a^m (systematic)	···	30
C_e	347	27
C_p	175	9
C_{pa}	-33	15
C_{dd}	26	27
C_{ml}	0	2
$\omega_p'(T_r)^m$ (mapping, tracking)	···	34
$\omega_p'(T_r)^m$ (calibration)	···	34
B_k	37	22
B_q	21	20
$\mu_p'(T_r)/\mu_B$	···	4
m_μ/m_e	···	22
Total systematic for $R_\mu'(T_r)$	···	76
Total for a_μ	572	139

$$a_\mu = \frac{\omega_a}{\tilde{\omega}_p'(T_r)} \frac{\mu_p'(T_r)}{\mu_B} \frac{m_\mu}{m_e} \qquad (T_r = 25\,^\circ\mathrm{C})$$

- external inputs from CODATA 2022

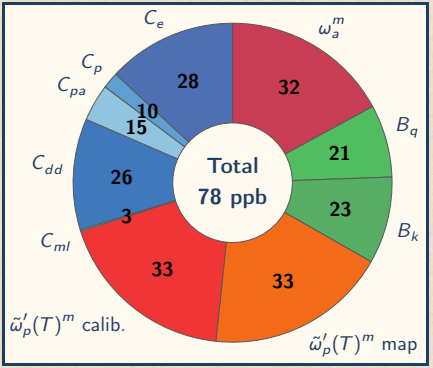


- total systematic < 100 ppb (design)
- systematics evenly distributed

Systematic corrections and uncertainties for final FNAL $R'_\mu(T_r)$

Quantity	Correction [ppb]	Uncertainty [ppb]
ω_a^m (statistical)		98
ω_a^m (systematic)		32
ω_a^m		103
C_e	374	28
C_p	174	10
C_{ml}		3
C_{pa}	-34	15
C_{dd}	24	26
$C_{\text{beam dynamics}}$	538	43
ω_a (statistical)		98
ω_a (systematic)		53
ω_a		111
$\tilde{\omega}'_p(T)^m$ (statistical)		4
$\tilde{\omega}'_p(T)^m$ (systematic)		47
$\tilde{\omega}'_p(T)^m$		48
B_q	21	21
B_k	37	23
$B_{\text{transient fields}}$	58	31
$\tilde{\omega}'_p(T)^m$ (statistical)		4
$\tilde{\omega}'_p(T)^m$ (systematic)		57
$\tilde{\omega}'_p(T)^m$		57
R_μ (statistical)		98
R_μ (systematic)	596	78
R_μ		125

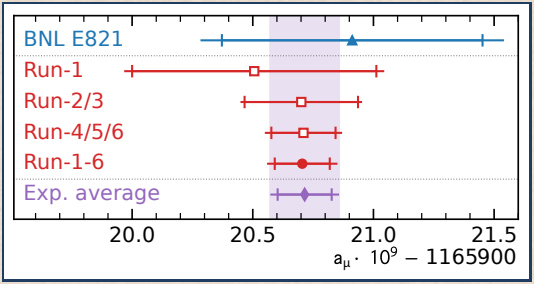
$$R'_\mu(T_r) = \frac{\omega_a}{\tilde{\omega}'_p(T_r)} \qquad (T_r = 25\,^\circ\text{C})$$



- total systematic < 100 ppb (design)
- systematics evenly distributed
- D.W.Hertzog & M.Hoferichter, Annu. Rev. Nucl. Part. Sci. 76 (2026) 343–368

Result

- results blinded by unknown offset in calorimeter DAQ sampling frequency
- collaboration approved result before unblinding on 20 May 2025 spherical water sample at $T_r = 25\,^{\circ}\mathrm{C}$
- FNAL Run 1 & 2/3 results values and systematic uncertainties revised according to Run 4/5/6 findings
- new W.A. of a_μ via combining all $R'_\mu(T_r)$'s (100% correlated systematics for FNAL measurements)
- PRL 135 (2025) 101802
- new: arXiv:2606.17323 [hep-ex], Final FNAL report on muon g-2, submitted 15 Jun 2026



a_μ FNAL $= 0.001165920705\ (148)\ [127\ \mathrm{ppb}]$
a_μ EXP $= 0.001165920715\ (145)\ [124\ \mathrm{ppb}]$

$R'_\mu(T_r)$ uncertainties

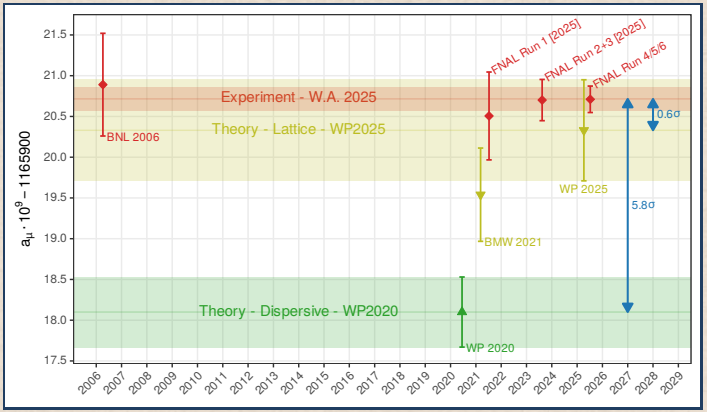
	stat. [ppb]	syst. [ppb]	total [ppb]
Run-1	434	159*	462
Run-2/3	201	78*	216
Run-4/5/6	114	76	137
Run-1-6	98	78	125

*revised

a_μ: $\oplus 22$ ppb external input systematics

Result

- results blinded by unknown offset in calorimeter DAQ sampling frequency
- collaboration approved result before unblinding on 20 May 2025 spherical water sample at $T_r = 25\,^{\circ}\mathrm{C}$
- FNAL Run 1 & 2/3 results values and systematic uncertainties revised according to Run 4/5/6 findings
- new W.A. of a_μ via combining all $R'_\mu(T_r)$'s (100% correlated systematics for FNAL measurements)
- PRL 135 (2025) 101802
- new: arXiv:2606.17323 [hep-ex], Final FNAL report on muon g-2, submitted 15 Jun 2026



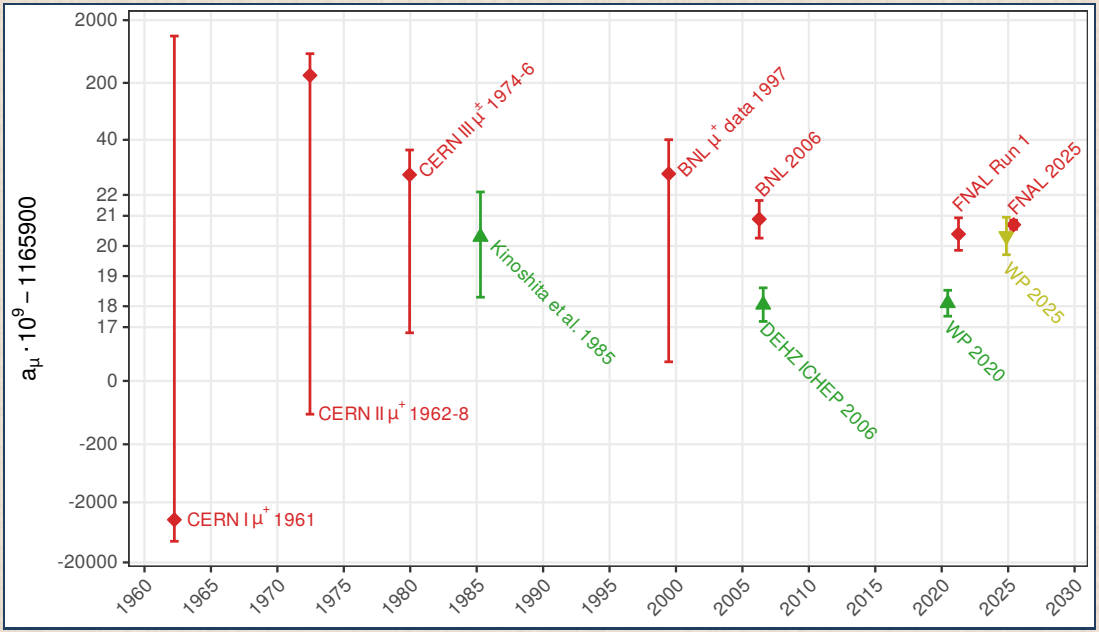
$R'_\mu(T_r)$ uncertainties

	stat. [ppb]	syst. [ppb]	total [ppb]
Run-1	434	159*	462
Run-2/3	201	78*	216
Run-4/5/6	114	76	137
Run-1-6	98	78	125

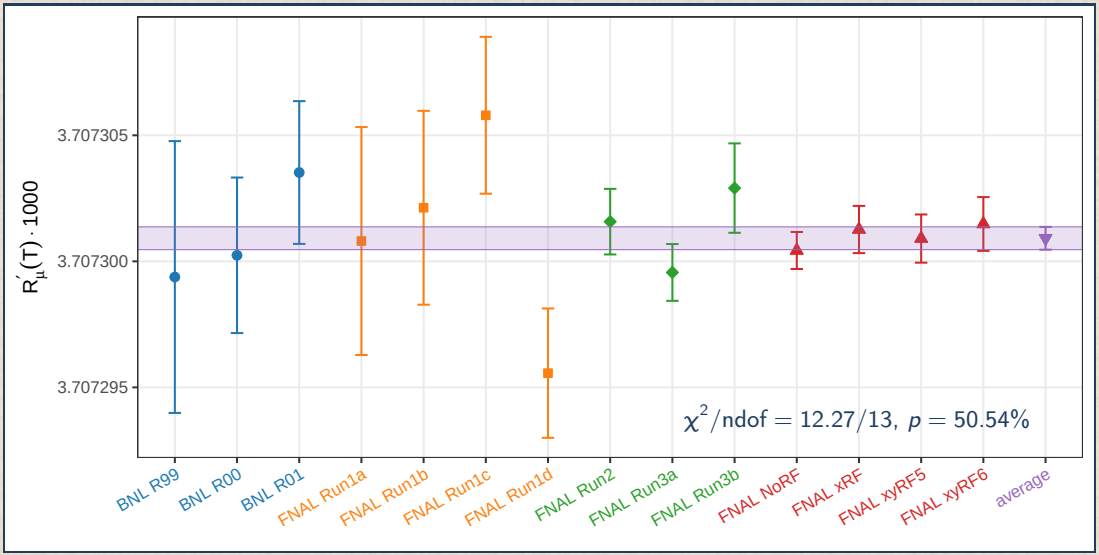
*revised

a_μ: $\oplus 22$ ppb external input systematics

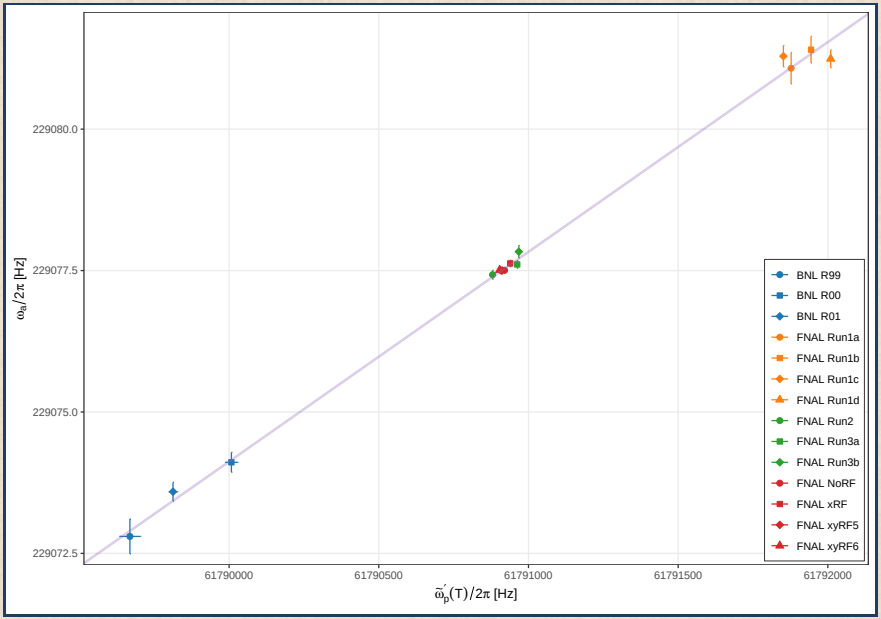
Long term perspective experimental consistency, 1961–2025



Consistency of BNL and FNAL datasets



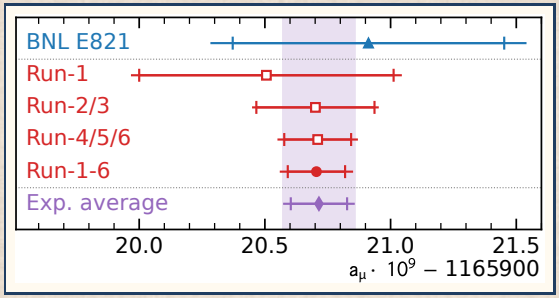
Consistency of BNL final report and FNAL datasets, ω_a vs. $\tilde{\omega}'_p(T_r)$



Conclusion

- most precise a_μ measurement
  probably for many years to come
- key ingredient of SM test
- tight constraint on New Physics models

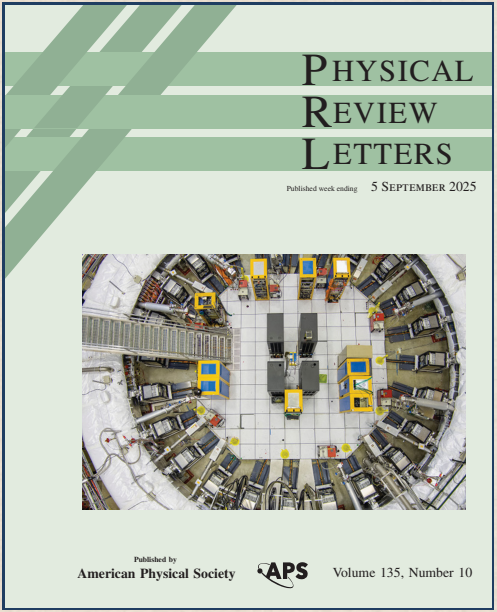




PRL 135 (2025) 101802
arXiv:2606.17323 [hep-ex], Final FNAL report on muon g-2, submitted 15 Jun 2026

Backup slides

PRL publication dated 2 Sep 2025



PRL Editors' Suggestion

04/09/2025, 13:35 Physical Review Letters - Volume 135 Issue 10

HIGHLIGHTED ARTICLES

FEATURED IN PHYSICS EDITORS' SUGGESTION

Measurement of the Positive Muon Anomalous Magnetic Moment to 127 ppb

D. P. Aguillard *et al.* (Muon $g-2$ Collaboration)

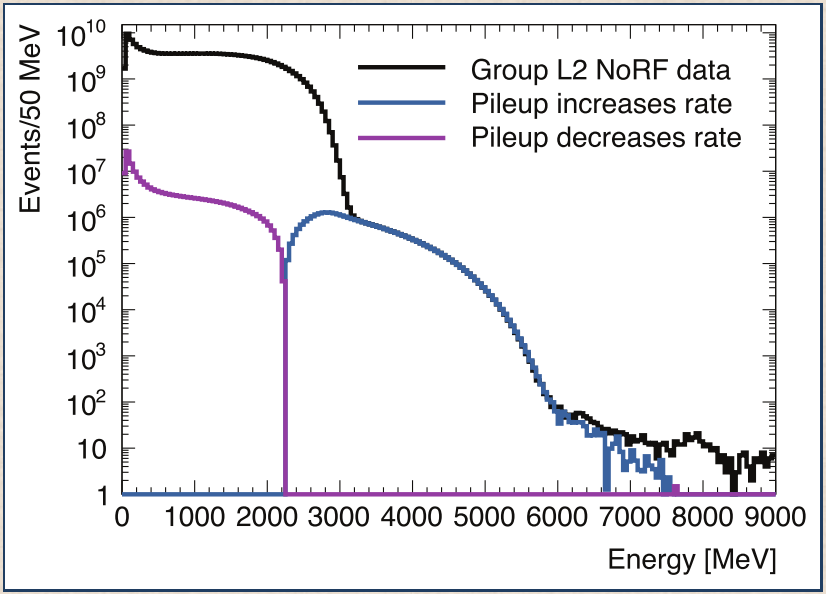
Phys. Rev. Lett. **135**, 101802 (2025) - Published 2 September, 2025



The final results from the Muon $g-2$ experiment agree with the latest predictions of the muon's magnetic properties—letting down hopes that the particle would upset the standard model's applecart.

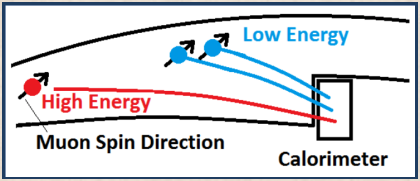
PRL 135 (2025) 101802

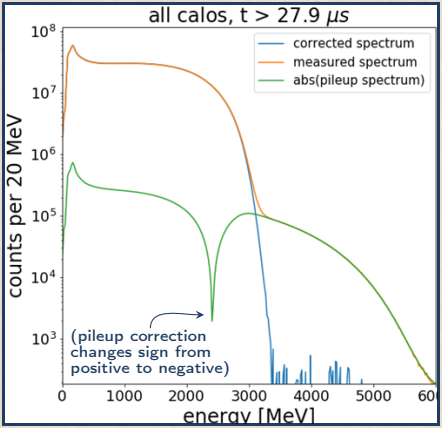
Pileup Run 4/5/6



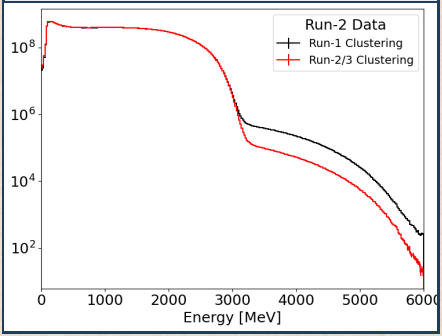
Pileup Run 2/3

- get pileup correction from data
  count hits in test window close to each existing hit
- series of improvements in Run 2/3 and Run 4/5/6
  - better reconstruction ⇒ reduced pileup hits
  - apply modeling of pileup built from real data hits
- estimated pileup statistically subtracted





reduced pileup in Run 2+3



Use bootstrap samples to estimate correlations between ω_a^m measurements

- for each dataset, build 200 bootstrap samples of same size
  by randomly selecting DAQ subruns with replacement [B. Efron, Annals Statist. 7 (1979)]
  (subruns are DAQ files, each containing around 37 K muon decays with energetic positrons in the calorimeters)
- for each analysis i, perform fits on 200 bootstrap samples $\Rightarrow \omega_a^m$ fit measurements $m_{i,b}$
- estimate ω_a^m covariance: $\mathrm{cov}(m_1, m_2) = \dfrac{\sum_b (m_{1,b} - \overline{m}_1)(m_{2,b} - \overline{m}_2)}{N_b - 1}$ with $\overline{m}_i = \dfrac{\sum_b m_{i,b}}{N_b}$
- expected residual variance $\sigma^2 (m_2 - m_1) = \sigma_1^2 + \sigma_2^2 - 2\rho\sigma_1\sigma_2$

bootstrap samples produced for most analyses

group	method	RF datasets
BU	T, A, RT, RA	No, x, xy5, xy6
EU	T, A, RT, RA	No, x, xy5, xy6
RE1	T, A	No, x, xy5, xy6
RE2	T, A	No, x, xy5, xy6
RE3	RA	No, x, xy5, xy6
RE4	SA	No, x, xy5, xy6
SJTU	T, A	No, x, xy5, xy6

correlations between Q-x vs. A-x & T-x analyses

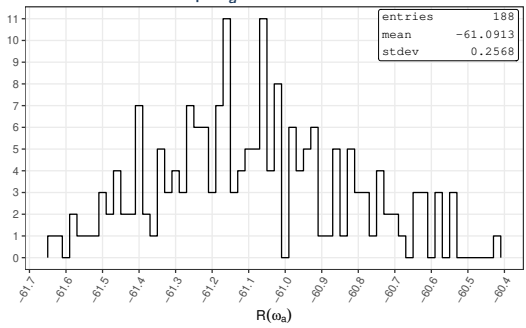
- bootstrap fits not performed for Q-x analyses
- reliable correlation evaluations using fits on 34 sub-samples of Run 4/5/6 sample

past evaluations of analyses' correlations

- also used alternative correlation estimates from dedicated Run 2/3 studies for cross-checks (partly outdated)

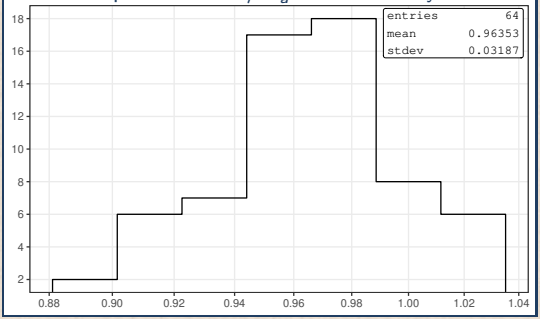
Bootstrap ω_a^m distribution width consistent with fit uncertainty

trimmed bootstrap ω_a^m distribution



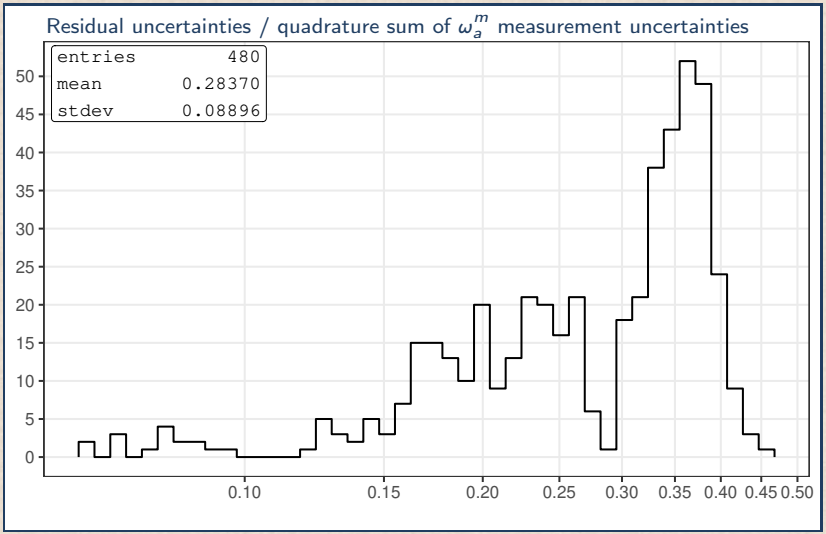
- removed $>3\,\sigma$ outliers of $m_{i,b}$ distribution

bootstrap RMS width / ω_a^m fit uncertainty



- bootstrap ω_a^m RMS width consistent with ω_a^m fit uncertainty when taking into account $3\,\sigma$ trimming

Residual uncertainty / total uncertainty



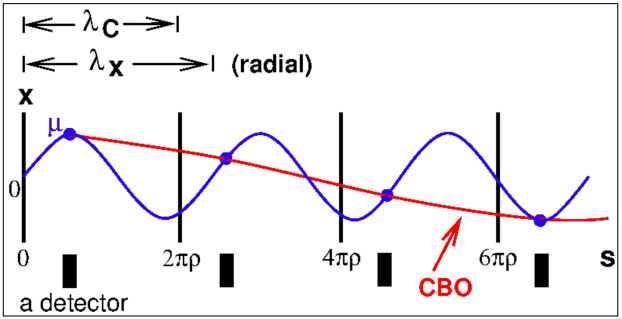
- large uncertainties: different methods (Q-A, Q-T, A-T)
- small uncertainties: ratio vs. non-ratio, different reconstructions

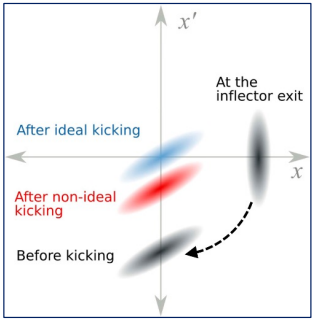
Beam dynamics frequencies

Physical frequency	Name	Expression	Frequency (MHz)	Period (μs)
Anomalous precession	f_a	$\frac{eB}{2\pi m_\mu} a_\mu$	0.229	4.37
Cyclotron	f_c	$\frac{v}{2\pi R_0}$	6.71	0.149
Horizontal betatron	f_x	$\sqrt{1-n}\, f_c$	6.34	0.158
Vertical betatron	f_y	$\sqrt{n}\, f_c$	2.20	0.453
Horizontal CBO	f_{CBO}	$f_c - f_x$	0.37	2.68
Vertical waist	f_{VW}	$f_c - 2f_y$	2.31	0.433

Expected beam dynamics frequencies for an effective field index $n = 0.108$.
The measured frequencies coincide at the 1% level.

Coherent Betatron Oscillation

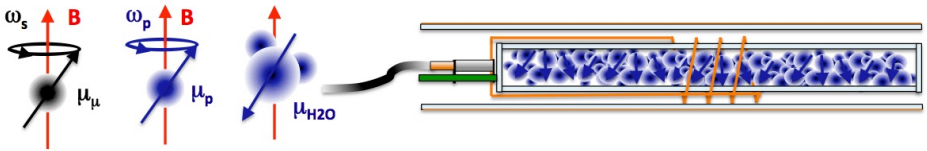




- Calo acceptance depends on muon radius at decay: coherent beam motion modulates e^+ time spectrum
- Radial betatron wavelength (blue line) $\neq$ circumference (cyclotron wavelength)
- Red line: apparent radial breathing in and out of beam at alias frequency $f_{\text{CBO}} = f_{\text{cyclotron}} - f_{\text{betatron}}$
- Effect dephases gradually, nearly cancels when all detectors added together

[D.Kawall, Sep 2023]

Absolute Field Measurement with Pulsed NMR



$$\omega_p'(T_R) \;=\; \omega_p^{\text{probe}} \left[1 + \frac{1}{\gamma_p'}\frac{d\gamma_p'}{dT}(T - T_R) + \left(\epsilon - \frac{4\pi}{3}\right)\chi_{\text{H}_2\text{0}}(T) \;+\; \delta_{\text{materials}}\right]$$

⇒ Determine B seen by muons from measurement of ω_p' of protons in spherical H_2O sample

- Complication: Diamagnetic shielding of electrons screens protons, *changes local* B, is T dependent, 10.36 ppb/C
- Complication: Very hard to make a spherical water sample
- Complication: magnetic susceptibility $\chi_{H_2O} \approx -0.721(2) \times 10^{-6}$ of water sample gives shape-dependent field perturbation: $\epsilon = 4\pi/3$ for a sphere, $\epsilon = 2\pi$ for cylinder $\perp \vec{B}$, 1.5 ppm shift !!!
- Complication: Best measurement of $\chi_{\text{H}_2\text{O}}$ comes from 1933! Working on update
- Complication: Magnetization of probe materials further perturbs field at site of protons

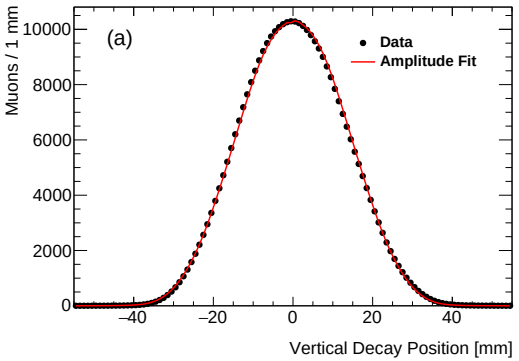
⇒ Determine total correction to 15 ppb accuracy or better using special calibration probes

[D.Kawall, Sep 2023]

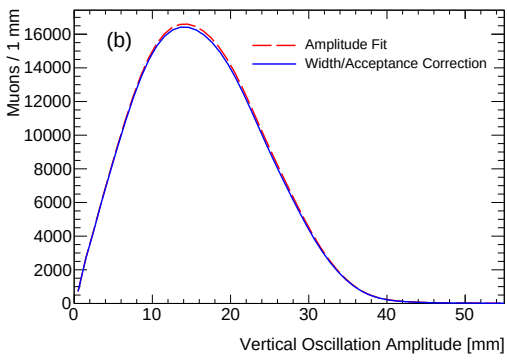
Pitch correction

- proportional to vertical muon velocity component (parallel to magnetic field)
- obtained using vertical spatial distribution of muons, measured by trackers

vertical decay-vertex distribution



vertical oscillation amplitude distribution



Phase changes over each fill

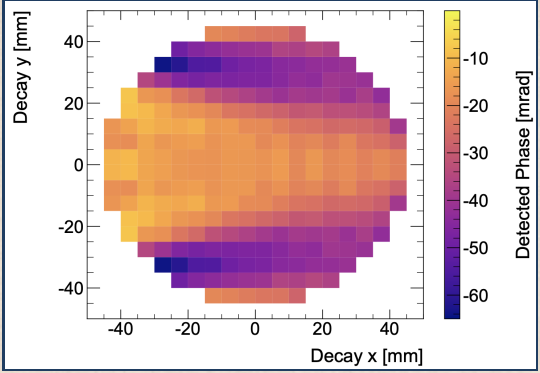
example: phase variation due to muon loss

- $N(t) = N_0 e^{-t/\tau_\mu}\,[1 + A\cos(\omega_a t + \varphi)]$ phase φ = muon spin-momentum angle at injection
- muon loss depends on momentum $\Rightarrow$ muon sample momentum varies $\bar{p} = \bar{p}(t)$
- single muon phase depends on momentum (because of production chain) $\bar{\varphi} = \bar{\varphi}(\bar{p})$
- at first order $\bar{\varphi}(t) = \bar{\varphi}_0 + \frac{\mathrm{d}\bar{\varphi}}{\mathrm{d}t} t = \bar{\varphi}_0 + \frac{\mathrm{d}\bar{\varphi}}{\mathrm{d}\bar{p}} \frac{\mathrm{d}\bar{p}}{\mathrm{d}t} t \simeq \bar{\varphi}_0 + \bar{\varphi}' t$
- muon rate modulation $\cos(\omega_a t + \bar{\varphi}(t)) \simeq \cos\left(\omega_a t + \bar{\varphi}_0 + \bar{\varphi}' t\right) = \cos[(\omega_a + \bar{\varphi}')t + \bar{\varphi}_0]$
  $\Rightarrow \Delta\omega_a = \bar{\varphi}'$
- note: muon loss phase effect is different and additional to muon loss effect on positron rate

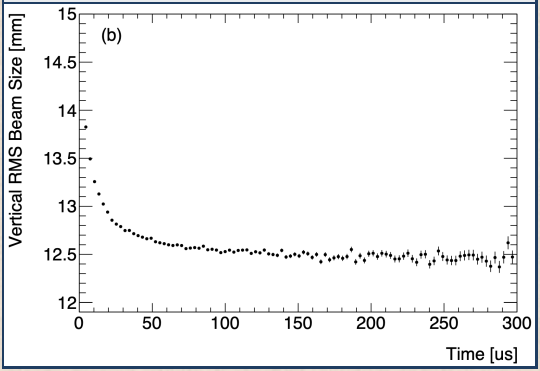
Phase-Acceptance correction

- effective phase variation due to variation of beam horizontal and vertical position and spread
- example: $\Delta\omega_a = \frac{d\varphi}{dt} = \frac{d\varphi}{dY_{RMS}} \cdot \frac{dY_{RMS}}{dt}$
- obtained with simulation
- measured with trackers and extrapolated to whole ring with beam dynamics simulations

phase as a function of muon position



variation of Y_{RMS}

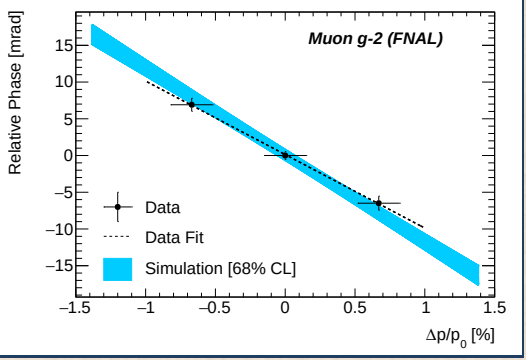


Differential decay corrections

- at $t = 0$, injected muons have a momentum distribution with a mean and spread
- at $t > 0$, average momentum increases because slower muons decay earlier
- phase change in fill due to variables correlated with momentum
  - horizontal position and angle (x, x')
  - vertical position and angle (y, y') (this is negligible)
  - time of flight from when muon polarization is selected to kicker hit
  - momentum itself

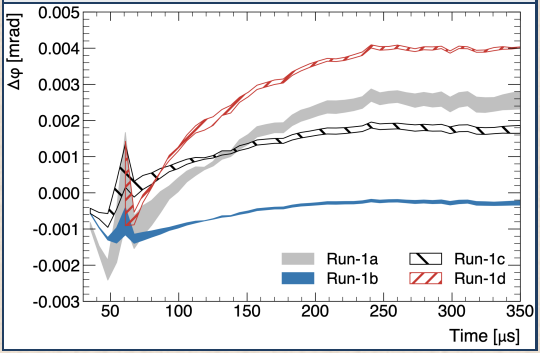
Lost muons phase-variation effect correction

measured and simulated $\varphi - p$ correlation



- muon phase depends on momentum
- muon population momentum changes because muon loss probability depends on momentum
- $\frac{d\varphi}{dp}$ measured on dedicated runs by varying magnetic field by -0.68%, +0.68%
- measurement consistent with simulation

estimated $\Delta\varphi(t)$ due to muon loss



- use delivery ring collimators to change the muon momentum distribution
- muon loss function of time and momentum fitted using simulation-inspired analytic function to model observed beam loss for different muon momentum distributions